Ncoa2 promotes CD8$^+$ T cell-mediated anti-tumor immunity by stimulating T cell activation via up-regulation of PGC-1α critical for mitochondrial function

Xiancai Zhong[1], Hongmin Wu[1], Ching Ouyang[2], Wencan Zhang[1], Yun Shi[1], Yi-Chang Wang[3], David Ann[3], Yousang Gwack[4], Weirong Shang[5] and Zuoming Sun[1]*

[1]Department of Immunology & Theranostics, Arthur Riggs Diabetes & Metabolism Research Institute, Beckman Research Institute of the City of Hope, Duarte, CA, 91010, USA

[2]Department of Computational and Quantitative Medicine, Beckman Research Institute, City of Hope Comprehensive Cancer Center, Duarte, CA 91010, USA

[3]Department of Diabetes Complication and Metabolism, Arthur Riggs Diabetes & Metabolism Research Institute, Beckman Research Institute of the City of Hope, Duarte, CA, 91010, USA

[4]Department of Physiology, David Geffen School of Medicine, UCLA, Los Angeles, CA, 90095, USA

[5]Department of Gynecology and Obstetrics, School of Medicine, Emory University, Atlanta, GA 30322, USA

* Corresponding author Zuoming Sun (zsun@coh.org)

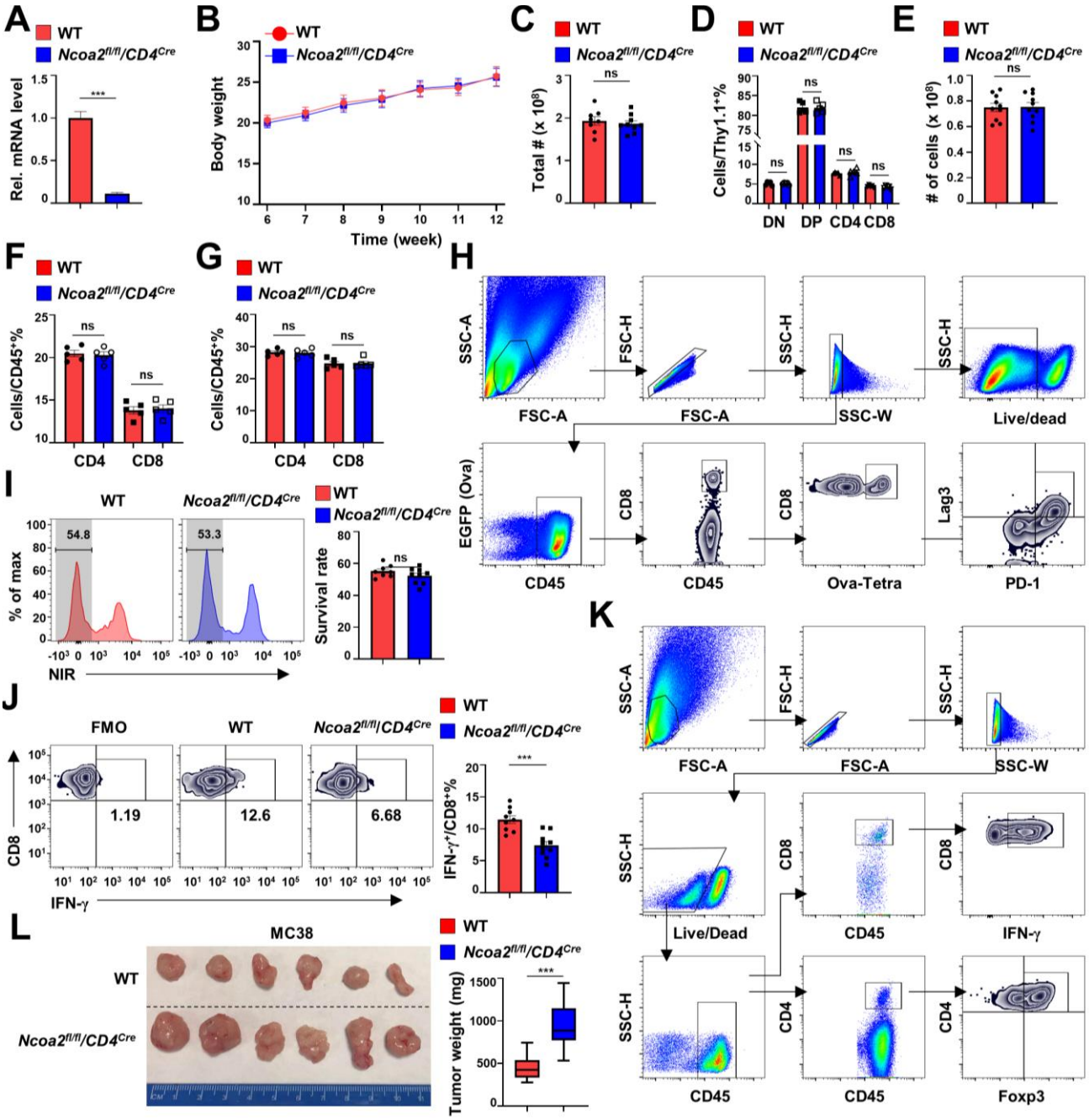
A
WT
Ncoa2fl/fl/CD4Cre
Rel. mRNA level
***
B
Body weight
Time (week)
C
Total # (x 10^8)
ns
D
Cells/Thy1.1+%
DN DP CD4 CD8
E
# of cells (x 10^8)
F
Cells/CD45+%
CD4 CD8
G
H
SSC-A
FSC-H
SSC-H
FSC-A
SSC-W
Live/dead
EGFP (Ova)
CD8
CD45
Ova-Tetra
Lag3
PD-1
I
% of max
54.8
53.3
NIR
Survival rate
J
FMO
1.19
12.6
6.68
IFN-γ
IFN-γ+/CD8+%
K
Live/Dead
IFN-γ
CD4
Foxp3
L
MC38
Tumor weight (mg)
M
CD8+/CD45+%
CD4+/CD45+%
N
IFN-γ+/CD8+%
O
IL-10+/CD8+%
P
PD-1+Tim3+/CD8+%
PD-1+Lag3+/CD8+%
Q
Foxp3+/CD4+%

Figure S1. (A) RT-qPCR analysis of *Ncoa2* (encoding SRC-2) mRNA in indicated $CD3^+$ T cells. (B) Body weight of WT and $Ncoa2^{fl/fl}/CD4^{Cre}$ mice (n = 12, 1:1 ratio for male and female). (C-D) Total thymocyte number (#) (C) and flow cytometric analysis of the percentage of $CD4^-CD8^-$, $CD4^+CD8^+$, $CD4^+$, and $CD8^+$ (D) of thymus from indicated mice. (E-G) Total splenocyte number (E) and flow cytometric analysis of $CD4^+$ and $CD8^+$ T cells in the spleen (F) or lymph node (G) from indicated 8-10-week-old mice. (H) Gating strategy for Figure 1C, D, and G. (I) Flow cytometric staining of dead cells by a near infrared dye (NIR). (J) Flow cytometric control of fluorescence minus one (FMO, left panel) and unstimulated $CD8^+$ T cells from tumors with full staining (middle and right panels) for determining gate boundary for IFN-γ. (K) Gating strategy for Fig. 1E and J. (L-Q) WT and $Ncoa2^{fl/fl}/CD4^{Cre}$ mice were subcutaneously implanted with 2 x 10^5 MC38 cancer cells and euthanized on day 14 (n=8-10, L-O) and day 19 post-engraftment for assessment (P-Q). (L) Tumor size (left panel) and weight (right panel) in indicated mice. (M) Flow cytometric analysis of the percentage of $CD8^+$ (left panel) and $CD4^+$ (right panel) among $CD45^+$ tumor-infiltrating lymphocytes (TILs) from indicated mice. (N-Q) Percentage of IFN-γ^+ (N), IL-10^+ (O), PD-1^+Tim3^+ and PD-1^+Lag3^+ (P) cells among tumor-infiltrating $CD8^+$ T cells, and percentage of Foxp3^+ cells among $CD4^+$ T cells in tumors in indicated mice. (L-M) Box plots show the median (central line), maximum, minimum (box ends), and outliers (extended lines). (A, C-G, I-J, O-Q) Data are shown as mean ± SEM. **P<0.01; ***P<0.001; ns, not significant (two-tailed unpaired Student's t-test).

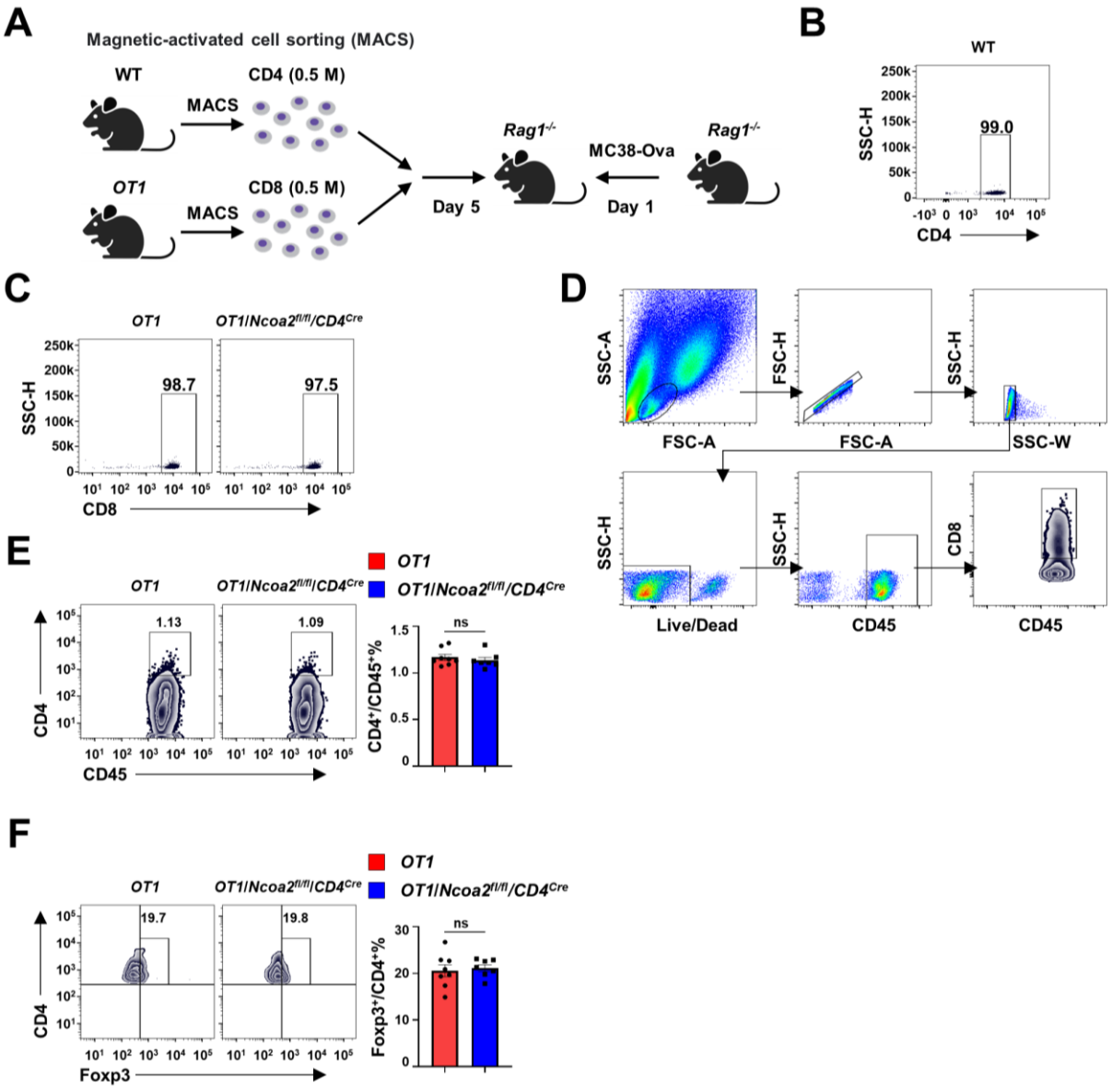

Figure S2. (A) Scheme of experimental procedure for tumor rejection using adoptively transferred *OT1* $CD8^+$ and WT $CD4^+$ T cells shown in Figure 2A. (B and C) Flow cytometric verification of the purity of magnetic cell sorting (MACS) naïve WT $CD4^+$ (B) and indicated *OT1* $CD8^+$ (C) T cells with >97% purity. (D) Gating strategy for Figures 2B and 2E. (E-F) Flow cytometric analysis of percentages of $CD4^+/CD45^+$ (E) and $Foxp3^+/CD4^+$ (F) shown in Fig. 2A-E. Data in (E-F) are shown as mean ± SEM. ns, not significant (two-tailed unpaired Student's t-test).

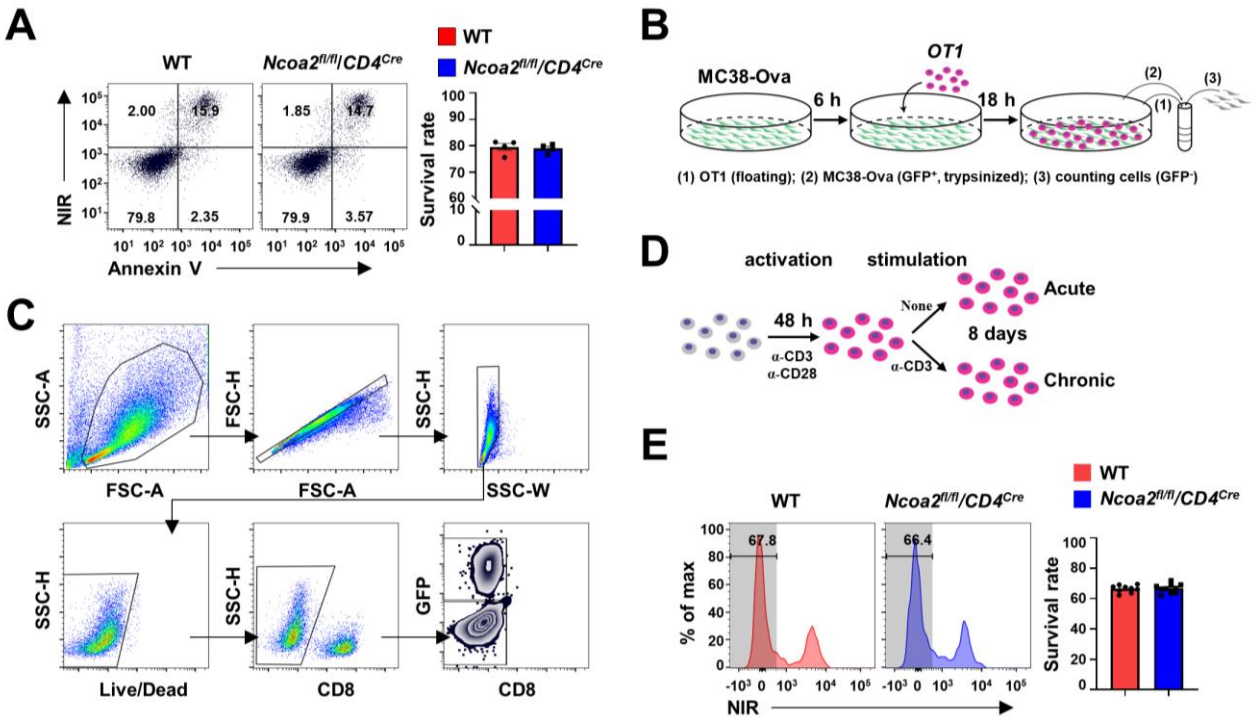

Figure S3. (A) Flow cytometric analysis of *in vitro* activated CD8$^+$ T cells from indicated mice for assessing cell survival by staining NIR dye and Annexin V. (B-C) Scheme for the experimental procedure measuring killing capacity of CD8$^+$ T cells (B) and gating strategy for Fig. 3E (C). (D) Scheme for acute and chronic activation of CD8$^+$ T cells for Figure 3F. (E) Flow cytometric analysis of cell survival of tumor infiltrated CD45.1-expressing WT and CD45.2-expressing *Ncoa2*$^{fl/fl}$*/CD4*^{Cre} CD8$^+$ cells shown in Fig. 3I-N.

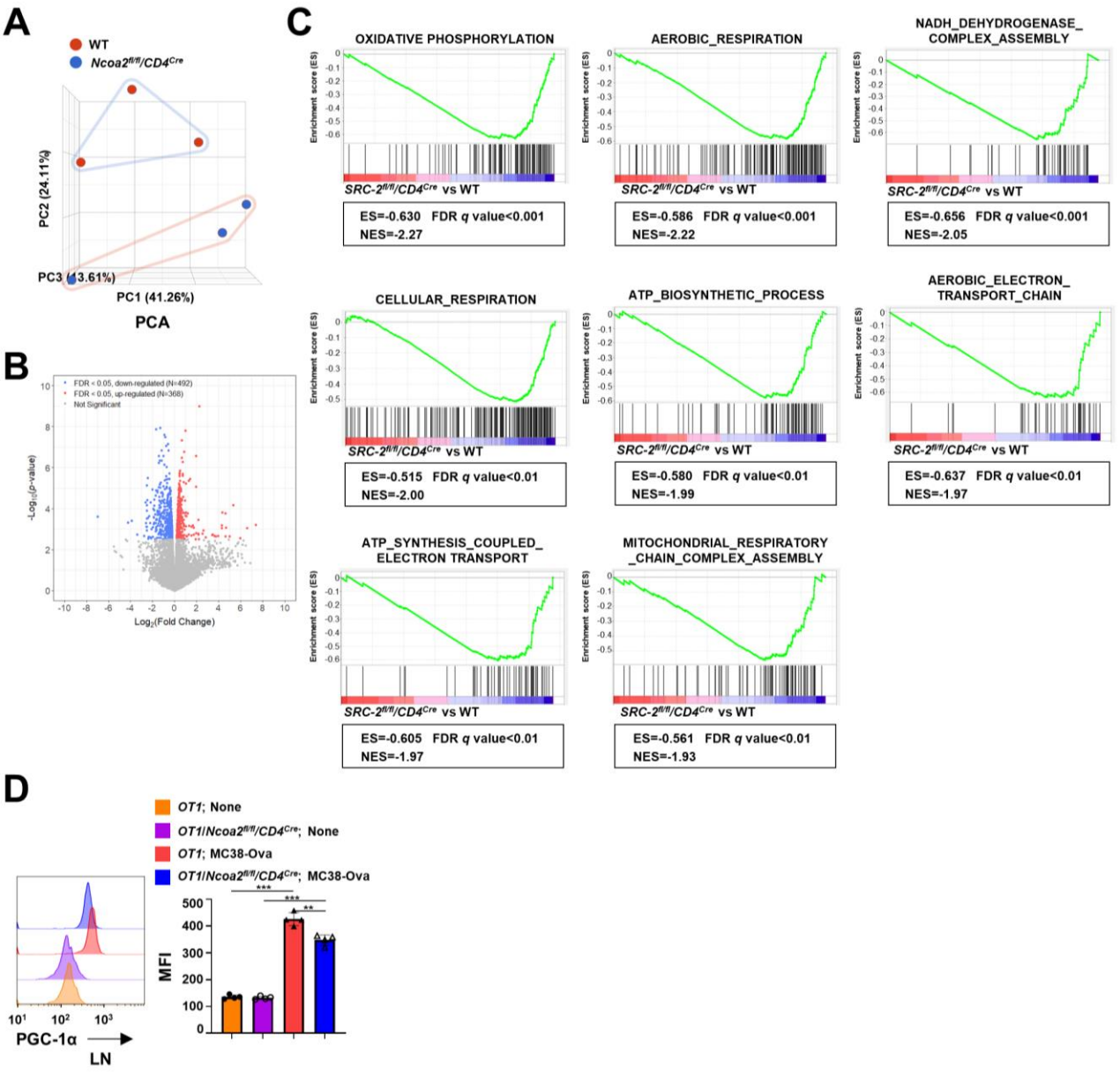

Figure S4. (A) Principal component analysis (PCA) of RNA-seq data. (B) Volcano plot showing upregulated or down-regulated DEGs [cut off at false discovery rate (FDR)<0.05]. (C) Gene set enrichment analysis (GSEA) plots of DEGs involved in mitochondrial metabolism when compared *Ncoa2*$^{fl/fl}$*/CD4*^{Cre} and WT CD8^{+} T cells. (D) Representative flow cytometric analysis (left panels) and mean fluorescence intensity (MFI) of PGC-1α in the CD8^{+} T cells from lymph node (LN) of indicated mice challenged without or with the challenge of MC38-Ova for 3 days. Data shown are mean ± SEM. ***P*<0.01; ****P*<0.001; ns, not significant (two-tailed unpaired Student's t-test).

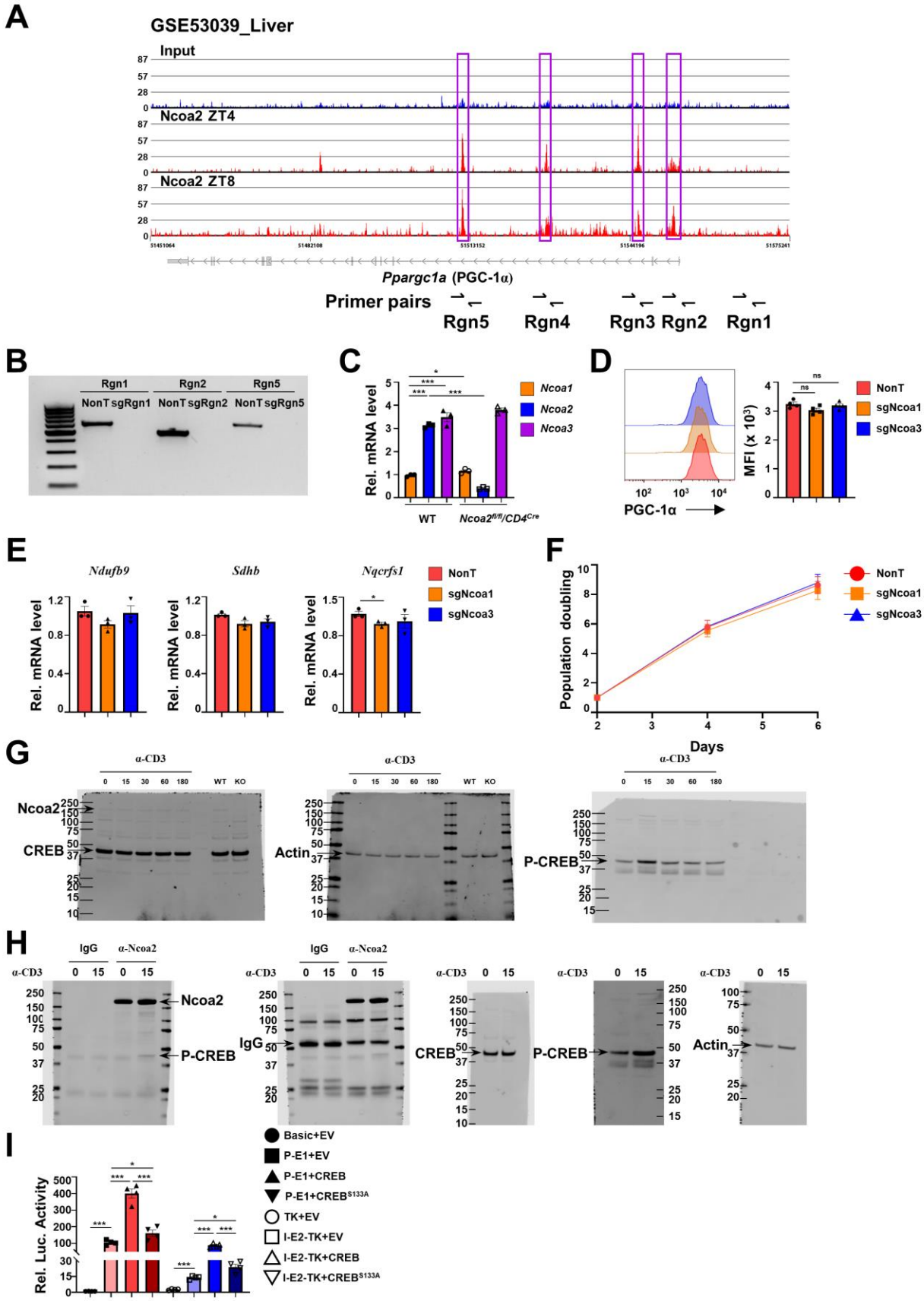
A
GSE53039_Liver
Input
Ncoa2 ZT4
Ncoa2 ZT8
Ppargc1a (PGC-1α)
Primer pairs
Rgn5
Rgn4
Rgn3
Rgn2
Rgn1
B
Rgn1
Rgn2
Rgn5
NonT sgRgn1
NonT sgRgn2
NonT sgRgn5
C
Rel. mRNA level
Ncoa1
Ncoa2
Ncoa3
WT
Ncoa2fl/fl/CD4Cre
D
PGC-1α
MFI (x 10³)
NonT
sgNcoa1
sgNcoa3
ns
E
Ndufb9
Sdhb
Nqcrfs1
Rel. mRNA level
NonT
sgNcoa1
sgNcoa3
F
Population doubling
Days
NonT
sgNcoa1
sgNcoa3
G
α-CD3
0 15 30 60 180 WT KO
Ncoa2
CREB
Actin
P-CREB
H
IgG
α-Ncoa2
α-CD3
0 15 0 15
Ncoa2
P-CREB
IgG
CREB
P-CREB
Actin
I
Rel. Luc. Activity
Basic+EV
P-E1+EV
P-E1+CREB
P-E1+CREB S133A
TK+EV
I-E2-TK+EV
I-E2-TK+CREB
I-E2-TK+CREB S133A

Figure S5. (A) ChIP-seq detected DNA-binding peaks of Ncoa2 at the *Ppargc1a* (PGC-1α) gene locus in liver tissues (GSE53039). Region (Rgn) 2-5 are the potential Ncoa2 DNA-binding regions at the *Ppargc1a* (PGC-1α) gene locus, whereas Rgn1 is the negative control of Ncoa2 DNA-binding region. (B) PCR analysis of Rgn2 and Rgn5 in sorted Cas9-expressing $CD8^+$ T cells that were transduced with non-targeting (NonT), or dual sgRNAs for deletion of Rgn2 or Rgn5. (C) Relative mRNA levels of *Ncoa1*, *Ncoa2*, and *Ncoa3* in OT1 and *OT1/Ncoa2*$^{fl/fl}$*/CD4*^{Cre} $CD8^+$ T cells activated *in vivo* by engraftment of MC38-Ova cancer cells for 3 days. (D-E) Flow cytometric analysis of PGC-1α (D) or qPCR analysis of expression of PGC-1α downstream mitochondrial genes, *Ndufb9*, *Sdhb* and *Nqcrfs1* (E) in Cas9-expressing $CD8^+$ T cells transduced with control NonT sgRNA, or sgRNAs that delete *Ncoa1* or *Ncoa3* genes. (F) Doubling of cell number over 6 days post-*in vitro* stimulation of indicated $CD8^+$ T cells shown in D. (G-H) Raw Western blot images of Fig. 5J (G) and Fig. 5K (H). (I) Relative luciferase activity from indicated reporter transfected into 293T cells together with expression plasmid for CREB or $CREB^{S133A}$ or control empty plasmid (EV).

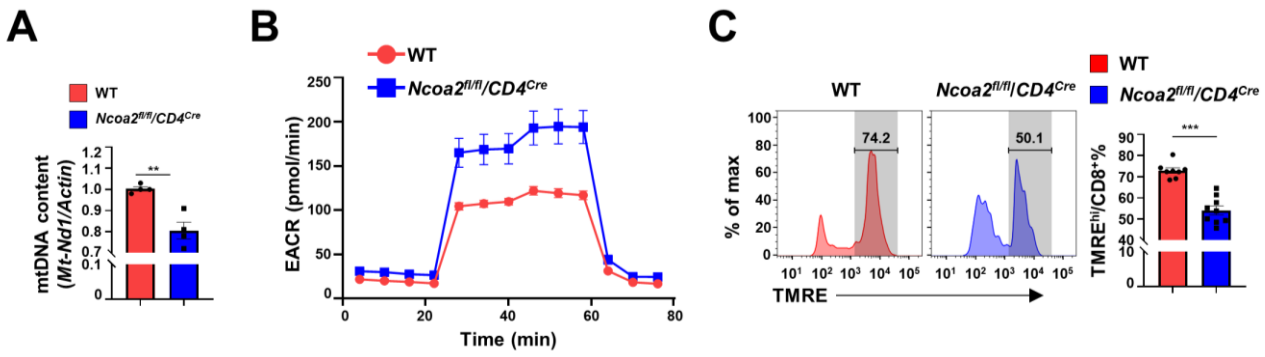

Figure S6. (A) RT-qPCR of mitochondrial DNA content (*mtNd1/Actin*) in WT and *Ncoa2*$^{fl/fl}$*/CD4*^{Cre} CD8^{+} T cells in vitro activated by α-CD3/CD28 antibodies for 24 h. (B) Seahorse analysis of extracellular acidification rate (ECAR) of glycolysis in WT and *Ncoa2*$^{fl/fl}$*/CD4*^{Cre} CD8^{+} T cells activated *in vitro*. (C) Flow cytometric analysis of mitochondrial membrane potential using tetramethylrhodamine, ethyl ester (TMRE).

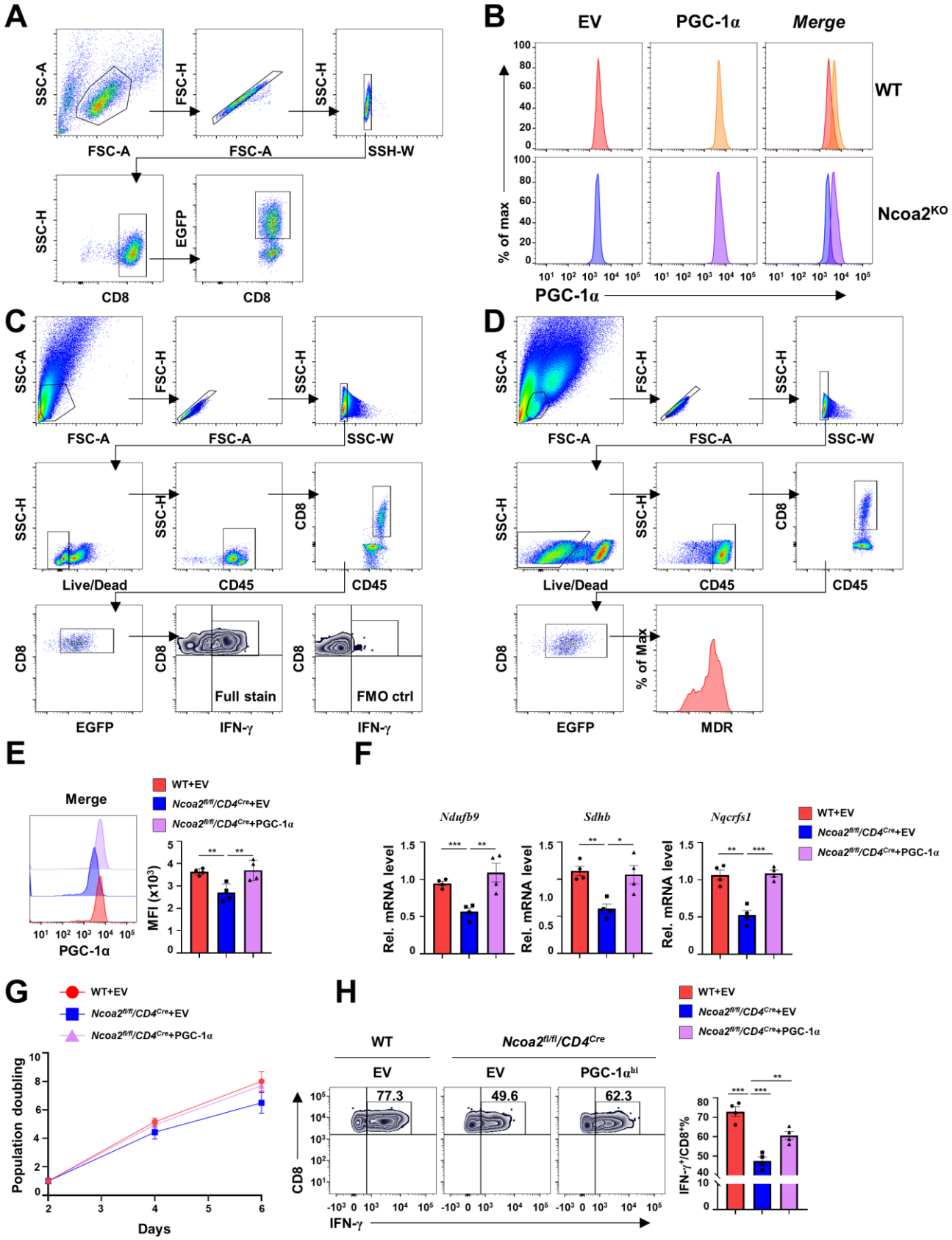
A
SSC-A
FSC-A
FSC-H
FSC-A
SSC-H
SSH-W
SSC-H
CD8
EGFP
CD8
B
EV
PGC-1α
Merge
WT
Ncoa2KO
% of max
PGC-1α
C
SSC-A
FSC-A
FSC-H
FSC-A
SSC-H
SSC-W
SSC-H
Live/Dead
SSC-H
CD45
CD8
CD45
CD8
EGFP
CD8
IFN-γ
Full stain
CD8
IFN-γ
FMO ctrl
D
SSC-A
FSC-A
FSC-H
FSC-A
SSC-H
SSC-W
SSC-H
Live/Dead
SSC-H
CD45
CD8
CD45
CD8
EGFP
% of Max
MDR
E
Merge
PGC-1α
WT+EV
Ncoa2fl/fl/CD4Cre+EV
Ncoa2fl/fl/CD4Cre+PGC-1α
MFI (x10³)
F
Ndufb9
Sdhb
Nqcrfs1
Rel. mRNA level
WT+EV
Ncoa2fl/fl/CD4Cre+EV
Ncoa2fl/fl/CD4Cre+PGC-1α
G
WT+EV
Ncoa2fl/fl/CD4Cre+EV
Ncoa2fl/fl/CD4Cre+PGC-1α
Population doubling
Days
H
WT
Ncoa2fl/fl/CD4Cre
EV
EV
PGC-1αhi
77.3
49.6
62.3
CD8
IFN-γ
WT+EV
Ncoa2fl/fl/CD4Cre+EV
Ncoa2fl/fl/CD4Cre+PGC-1α
IFN-γ+/CD8+%

Figure S7. (A) Gating strategy for Fig. 7B. (B) Representative flow cytometric analysis of PGC-1α in indicated $CD8^+$ T cells transduced with retrovirus expressing GFP alone (EV) or with PGC-1α. (C) Gating strategy for Fig. 7C and a FMO control was provided for determining gate boundary. (D) Gating strategy for Fig. 7D. (E-H) WT and *Ncoa2*$^{fl/fl}$*/CD4*^{Cre} $CD8^+$ OT1 cells were retrovirally transduced GFP alone (EV), whereas *Ncoa2*$^{fl/fl}$*/CD4*^{Cre} $CD8^+$ T cells were transduced with adjusted amount of PGC-1α expressing virus so that PGC-1α levels were equivalent to that of WT, indicated by E and analysis of PGC-1α downstream mitochondrial genes in cells shown in E. (G) Cell number doubling time in cells shown in E. (H) Percentage of IFN-γ^+ cells among indicated $CD8^+$ T cells shown in E after adoptively transferred to *Rag1*$^{-/-}$ mice challenged with MC38-Ova cancer cells for 3 days.

Table S1. List PCR primer sequences

RT-qPCR		
Gene	**Forward primer**	**Reverse primer**
Ncoa1	CCCTCAGTCAATCCTGGTATCT	CTGGCACACTGTCCTTCTTC
Ncoa2	GGCAGGTTTGGTGGTTCT	TTGCGAGGGACTGTTCATTT
Ncoa3	CAGAATCCAGTGGAGAGTTCAG	CTCTTTGGCAAGCACATCAC
Ppargc1a	TATGGAGTGACATAGAGTGTGCT	CCACTTCAATCCACCCAGAAAG
Ndufb9	GGTACTTTGCTTGCTTGATGAGA	TGGGAAGATATACGGCTGAGG
Sdhb	AATTTGCCATTTACCGATGGGA	AGCATCCAACACCATAGGTCC
Uqcrfs1	GAGCCACCTGTTCTGGATGTG	GCACGACGATAGTCAGAGAAGTC
Rgn1	GCCTATGAGATCCACGGAAAG	GTCTCCTTGGCAGTAGAGAATG
Rgn2	GGATCTTTGCTATTTGCCTGTT	GCTTTGAATGCCACCAACTC
Rgn3	GCAAAGGGTAAGGTCCTATGT	CACTAGAGGGCAAAGAGTGAG
Rgn4	CCACAGATTAGGAGTGTAGAAGTTAG	GAGGAAGAAGGGCAATCACA
Rgn5	ATCTTTGAGCCCTGAGTGAAC	AGCTGGGAGCAGTAGTGATA
Hbb	GCTCTGGGTACTCCCTCTGA	GCAAATGTGTTGCCAAAAAG
Regular PCR		
Gene	**Forward primer**	**Reverse primer**
Rgn2	TCTTTGCTATTTGCCTGTTTTGG	AGCTCCCGAATGACGCCAGTCAA
Rgn5	CTGAGAGTGCCAAGTTCAACAGC	GCGATAGCAAGTGGGAAATAACAGC

Table S2. List of gRNA sequences

gRNA	**Forward primer**
Ncoa1	GAATGGCCTCGGTCGTCGG
Ncoa3	ATCTTGGCGACCTCCGCTG
NonT #1	AAACTCGCCCGCGTCATAT
NonT #2	AAAGTACCCGCGCGTACGA
Rgn2 #1	GCAGGGCTCCGGTTTAGAGT
Rgn2 #2	ACTGGGGACTGTAGTAAGAC
Rgn5 #1	ACACAGATTGGAAATCGTAT
Rgn5 #2	AATGCATGCCATCACGTTGG